

## Detailed Investigation of the Divertor Radiation in ASDEX Upgrade

J.C. Fuchs, J. Gafert, A. Herrmann, K.F. Mast, and the ASDEX Upgrade Team

MPI für Plasmaphysik, EURATOM Association, 85748 Garching, Germany

### Introduction

A detailed knowledge of the radiation distribution in the divertor is necessary in order to increase and control the divertor radiation with the aim of reducing the power load on the divertor plates. Therefore, radiation losses in the ASDEX Upgrade divertor IIb and their dependence on various parameters have been investigated for several ITER relevant scenarios.

Radiation in ASDEX Upgrade is measured by 100 bolometers mounted in 7 cameras around the plasma, which allow to reconstruct the radiation distribution in the divertor and X-point region as well as in the main plasma. Since there may be closely located radiation structures especially in the divertor region which are too small to be detected under normal circumstances by the bolometers due to their limited spatial resolution, the plasma shift technique has been applied in order to reveal these structures. With this method, the plasma is shifted vertically for some centimeters, such that the region of interest is moved over one or more bolometer lines of sight. Assuming that the plasma does not change significantly during the shift, one can infer such structures from the time evolution of the measured line integrals and increase the spatial resolution for the tomographic reconstruction of the radiation distribution. Although it is a challenge for the plasma control to shift the plasma while keeping all parameters constant, these experiments were successfully carried out at ASDEX Upgrade for different scenarios.

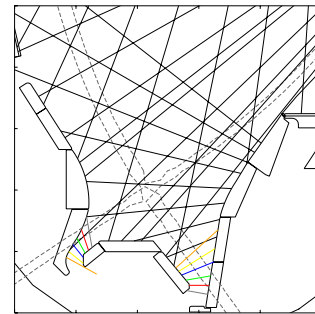


Fig. 1: Bolometer lines of sight in the ASDEX Upgrade divertor. The coloured lines of sight correspond to the line integrals from Fig.2, the dashed lines indicate the position of the separatrix during the plasma shift.

### Radiation pattern

The time evolution of the measured bolometers line integrals in the inner and outer divertor during the plasma shift as a function of the distance of the line of sight to the strikepoint can be seen in Fig. 2 for a shot with 7.5 MW neutral beam injection power,  $I_p=1$  MA,  $n_e=1\cdot 10^{20} \text{ m}^{-3}$ ,  $q_{05}=4.6$ . The curves for adjacent lines of sight overlap, thus indicating that for

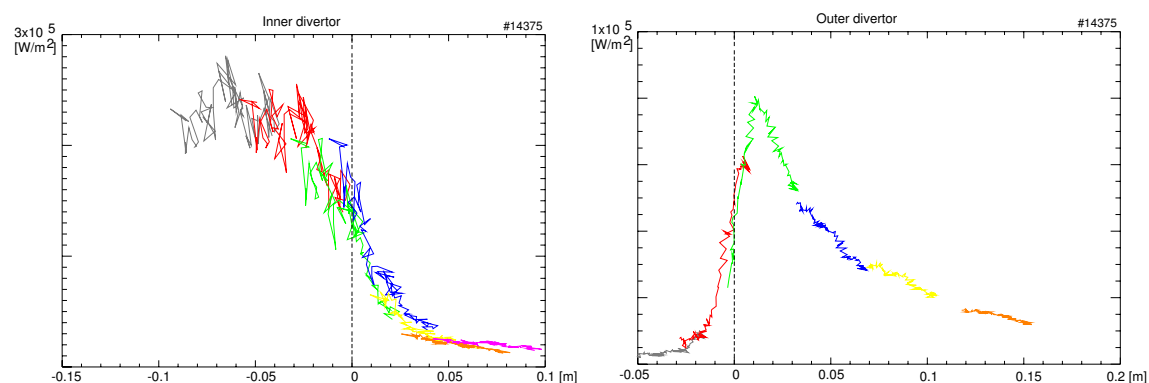


Fig. 2: Measured line integrals of the divertor bolometers during the plasma shift as a function of the distance of the line of sight to the strikepoint for the inner (left) and outer (right) divertor. Different colors denote different lines of sight, which are shown in Fig. 1.

the chosen time interval the radiation pattern in the divertor does not change significantly during the shift.

It can be seen, that in the outer divertor the maximum of the radiation is located in a narrow region near the strikepoint, whereas in the inner divertor the radiation is much higher and distributed over a broader area.

From the time evolution of the divertor bolometer shown in Fig. 2 as well as of the other bolometers, several virtual bolometer channels can be constructed and used together with the measured line integrals for the reconstruction of the radiation profile. The reconstruction is done with the ‘Anisotropic Diffusion Model Tomography’ algorithm, which is based on the fact that the variation of the radiation emissivity along magnetic field lines is much smaller than perpendicular to them. This behavior is described by an anisotropic diffusion model with different values of the diffusion coefficients  $D_{\parallel}$ ,  $D_{\perp}$  along and perpendicular to the magnetic field lines [1].

The resulting radiation pattern in the divertor is shown in Fig. 3. The radiation peak near the outer strikepoint is clearly seen with a radiation density of up to  $15 \text{ MW/m}^3$ . In the inner divertor we find a broader distribution of the radiation from the strikepoint to the X-point, however due to some broken bolometer channels the width of this radiation band could not be reconstructed with the same precision as formerly in divertor II [2].

The measured radiation in the divertor can be compared with the measurements of two arrays of chords which were equipped with CIII and  $H_{\alpha}$  filters. These arrays have roughly the same location and viewing direction as the corresponding bolometer cameras, but a much better spatial resolution (ca. 5mm) [3]. Fig. 4 shows a comparison of the measured CIII and  $H_{\alpha}$  radiation in the inner and outer divertor for a single time point with the time evolution of the bolometer line integrals, again versus the distance of the line of sight to the strike point.

It shows that the radiation measured by the bolometers is dominated by carbon radiation, and that the narrow radiation peak near the outer strike point is smoothed out by the bolometers due to the opening angle of the bolometer lines of sight.

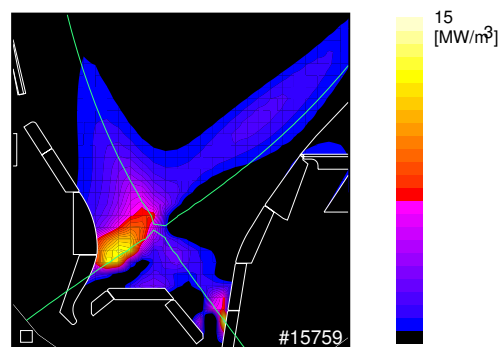


Fig. 3: Reconstructed bolometric radiation distribution using virtual lines of sight constructed from the time evolution of the bolometer line integrals during the plasma shift (for an identical repeat of the shot from Fig. 1)

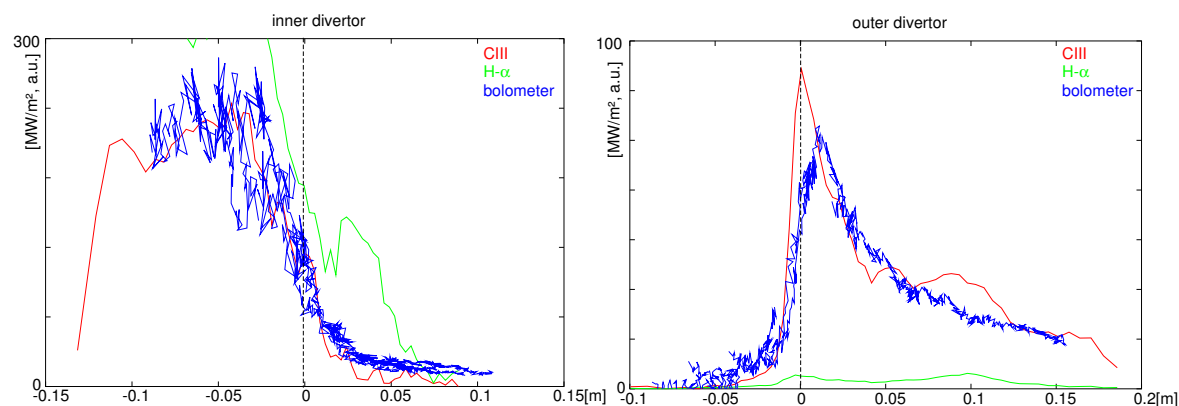


Fig. 4: Comparison of CIII radiation (red),  $H_{\alpha}$  radiation (green), and radiation measured by bolometers. Whereas the CIII and  $H_{\alpha}$  radiation is taken for one time point, the bolometer radiation comes from the time evolution of the line integrals during the plasma shift (see Fig. 2). (The CIII and  $H_{\alpha}$  line integrals are not calibrated.)

The measured CIII radiation from the mentioned arrays can be used together with the recording of a tangential viewing CCD camera which was equipped with a CIII filter in order to reconstruct the distribution of the CIII radiation. The result is shown in Fig. 5, which in comparison with the bolometer radiation distribution from Fig. 3 again shows that in the outer divertor the bolometer radiation is dominated by carbon radiation. B2–Eirene modelling of the radiation band in the inner divertor showed that the radiation in this band is mainly caused by  $H_{\alpha}$  radiation directly at the strikepoints, followed by C-II, CIII and C-IV radiation towards the X-point [2]. In Fig. 5 only the CIII radiation is shown, whereas the bolometer radiation in Fig. 3 is integrated over a large spectral range.

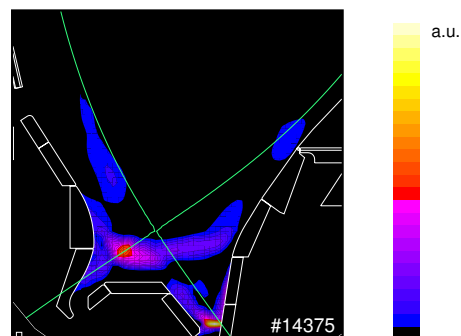


Fig. 5: Reconstructed distribution of the CIII radiation from a tangential viewing CCD camera for an comparable shot to that of Fig. 3.

### Dependence of the radiation distribution on plasma parameters

When looking for the dependence of the radiation distribution in the divertor on plasma parameters one finds that the distribution is nearly independent of the heating power, but the radiation is scaled with the heating power, as it used to be in the former divertor II [4]. On the other hand, the main chamber electron density and the neutral gas density in the divertor have a significant influence on both the radiation level and the distribution. With increasing density, it can be seen that the maximum of radiation departs from the strikepoint as the plasma detaches and finally a marfe is formed.

However, in most cases the main chamber density and the neutral gas density in the divertor vary not independently, so that it is difficult to distinguish the influence of these parameters on the radiation distribution. Therefore, the following example shows a shot, where the line averaged electron density in the main chamber was kept constant during the plasma shift, while the neutral gas density in the divertor increases with three different plateaus, and the edge density also increases. Fig. 6 shows how with increasing neutral gas density the maximum of the radiation departs from the strikepoint and the peak becomes smaller and broader.

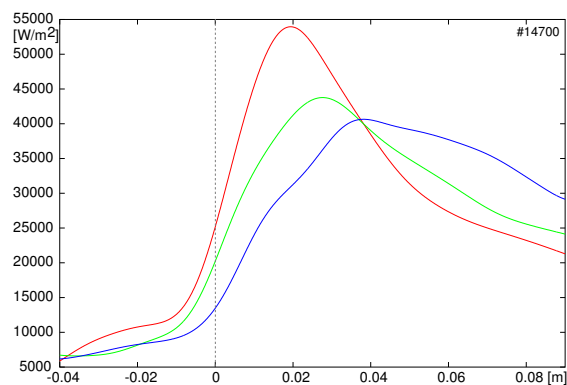


Fig. 6: Dependence of the radiation on the neutral gas density: For constant line averaged electron density in the main chamber ( $5.8 \cdot 10^{19} \text{ m}^{-3}$ ) the line integrals of radiation in the outer divertor as a function of the distance to the strikepoint are shown for three levels of neutral gas density in the divertor:  $4.7$  (red),  $5.3$  (green),  $6.0$  (blue)  $\cdot 10^{20} \text{ m}^{-3}$ .

### Comparison of Divertor IIb with Divertor II

Comparing the radiation distribution and radiation levels in the former divertor II and the present divertor IIb in ASDEX Upgrade, it was found that the fraction of radiation in the divertor is similar for both divertors for low triangularity configurations, whereas for high triangularities there is slightly less radiation in divertor IIb [5]. The power load on the target plates has correspondingly slightly increased for the divertor IIb.

Comparing the time evolution of the line integrals of radiation in the inner and outer divertor during plasma shifts of similar shots in divertor II and divertor IIb suggests, that in the outer divertor the radiation is now even closer located to the strikepoint than in divertor II, and the peak is higher and narrower in the outer divertor, whereas the distribution is similar in the inner divertor.

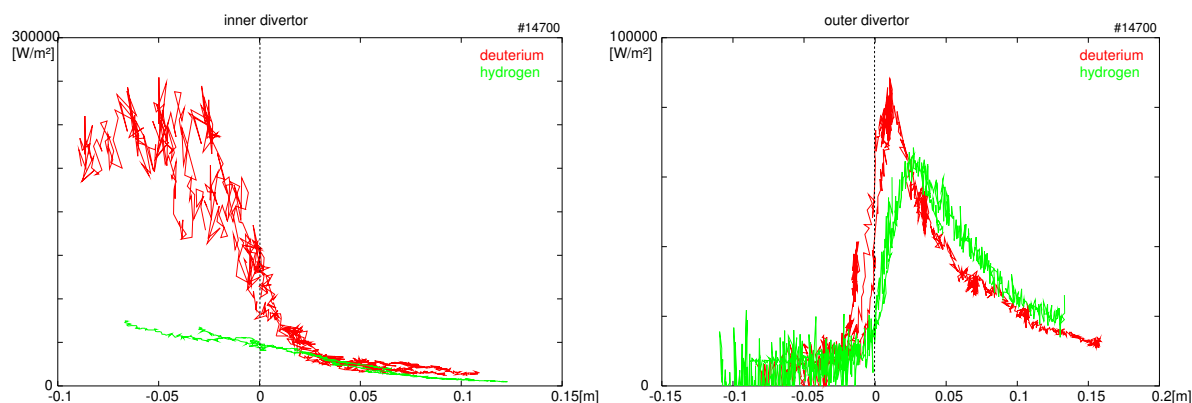


Fig. 7: Time evolution of the bolometer line integrals in the inner (left) and outer (right) divertor during the plasma shift as a function of the distance to the strikepoint for deuterium (red) and hydrogen (green) plasmas.

### Isotope dependence

The species of the main plasma gas (deuterium, hydrogen, helium) has a large influence on the radiation distribution. Fig. 7 shows the time evolution of the bolometer line integrals in the inner and outer divertor during a plasma shift for similar shots in deuterium and hydrogen plasmas. It can be seen, that in the outer divertor the radiation levels are similar, but the radiation is more located at the strikepoint in deuterium plasmas and further away in hydrogen plasmas. Results from the former divertor II also show, that in helium plasmas the maximum of radiation is even further away from the strikepoint. In the inner divertor however the radiation level is drastically reduced in hydrogen plasmas. These results are also proved by the CIII and  $H_{\alpha}$  measurements of the spectroscopic arrays mentioned earlier. The resulting bolometric radiation distribution is shown in Fig. 8.

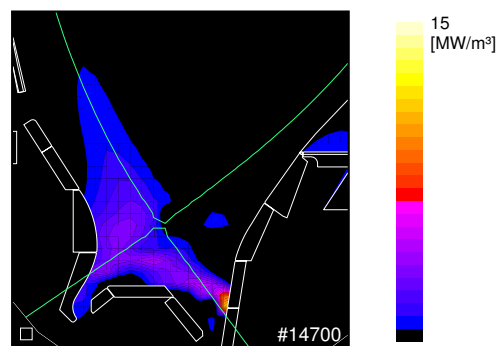


Fig. 8: Bolometric radiation distribution in the divertor for a hydrogen plasma.

### Conclusions

The radiation distribution in the divertor IIb of ASDEX Upgrade was investigated in detail using the plasma shift technique. Assuming that the plasma does not change significantly during the shift, one can infer small structures in the radiation distribution from the time evolution of the measured line integrals and increase the spatial resolution for the tomographic reconstruction of the radiation distribution.

It could be shown that in the outer divertor the radiation is closely located to the strikepoint, whereas the distribution is broader in the inner divertor. Comparison with spectrometers and measurements from CCD cameras equipped with different filters show that the radiation measured by bolometers is dominated by carbon. The distance of the radiation peak in the outer divertor and its width depend strongly on the main chamber and divertor density, but not on the heating power. For hydrogen plasmas, a strong reduction of the radiation was found in the inner divertor due to a reduction of carbon in that region.

### References

- [1] J.C. Fuchs, K.F. Mast, A. Herrmann, K. Lackner et al., *Contrib 21st EPS*, (1994) 1308ff
- [2] A. Kallenbach, M. Kaufmann, et al, *Nuclear Fusion* **39**(1999), 901ff
- [3] J. Gafert, et al, this conference
- [4] J. C. Fuchs, D. Coster, A. Herrmann, A. Kallenbach, K. F. Mast, et al, *J. Nucl. Mater.* **290-293**(2001), 501ff
- [5] R. Neu, et al, *Plasma Phys. Control. Fus.* **44**(2002), 1021-1029